Experimental Study on Vortex-Induced Vibration of Floating Circular Cylinders With Low Aspect Ratio and Different Free-End Corner Shapes

Conference Paper · June 2018

DOI: 10.1115/OMAE2018-77218

6 authors, including:

Rodolfo Trentin Gonçalves
The University of Tokyo
92 PUBLICATIONS **493** CITATIONS
SEE PROFILE

Keigo Sakata
The University of Tokyo
2 PUBLICATIONS **0** CITATIONS
SEE PROFILE

Dênnis Gambarine
University of São Paulo
5 PUBLICATIONS **8** CITATIONS
SEE PROFILE

Gustavo R S Assi
University of São Paulo
60 PUBLICATIONS **503** CITATIONS
SEE PROFILE

Proceedings of the ASME 2018 37th International Conference on Ocean, Offshore and Arctic Engineering
OMAE2018
June 17-22, 2018, Madrid, Spain

OMAE2018-77218

EXPERIMENTAL STUDY ON VORTEX-INDUCED VIBRATION OF FLOATING CIRCULAR CYLINDERS WITH LOW ASPECT RATIO AND DIFFERENT FREE-END CORNER SHAPES

Rodolfo T. Gonçalves[1]
(goncalves@edu.k.u-tokyo.ac.jp)

Keigo Sakata[1]
(sakata@s.otpe.k.u-tokyo.ac.jp)

Dennis M. Gambarine[2]
(dgambarine@technomar.com.br)

Murilo M. Cicolin[3]
(mmcicolin@gmail.com)

Shinichiro Hirabayashi[1]
(hirabayashi@edu.k.u-tokyo.ac.jp)

Gustavo R. S. Assi[4]
(g.assi@usp.br)

[1]Department of Ocean Technology, Policy, and Environment
School of Frontier Sciences, The University of Tokyo, Kashiwa-shi, Chiba, Japan

[2]Technomar Engenharia Oceânica, São Paulo, SP, Brazil

[3]Department of Mechanical Engineering
[4]Department of Naval Architecture and Ocean Engineering
Escola Politécnica – University of São Paulo
São Paulo, SP, Brazil

ABSTRACT

Experiments regarding vortex-induced vibration (VIV) on floating circular cylinders with low aspect ratio, $L/D = 0.5$, and different free-end conditions were carried out in a recirculation water channel. The floating circular cylinders were elastically supported by a set of linear springs to provide low structural damping on the system. Four different free-end corner shape conditions were tested, namely $r/R = 0.0$, 0.25, 0.5 and 1.0; where r/R is the relation between chamfer rounding radius, r, and the radius of cylinder, R. These different free-end conditions were selected to promote changes in the structures shedding around the free end of the cylinder. The aims were to understand the free-end effects on the VIV of floating circular cylinders with very low aspect ratio. The range of Reynolds number covered 2,800 < Re < 55,400. All the results presented here complement the work presented previously for a floating circular cylinder with $L/D = 2.0$ by Gambarine *et al.* (2016) [6] - Experimental study of the influence of the free end effects on vortex-induced vibration of floating cylinder with low aspect of ratio, OMAE2016-54623. The present results showed that the amplitudes in both directions were the highest for the semi-sphere case, $r/R = 1.0$. The amplitudes were almost the same for the other radius values, $0.0 \leq r/R \leq 0.5$; in which the maximum amplitudes decreased with increasing the corner radius. A critical value, $L/D_{crit} = 0.5$, in which only the free-end structures affect the VIV behavior of the cylinder piercing the free-surface could be stated. The conclusion was that the cylinder free-end affects the VIV behavior for cylinders with very low-aspect ratio.

Keywords: vortex-induced vibration (VIV), low aspect ratio, free-end corner shapes, floating circular cylinder

1. INTRODUCTION

The study on the fluid flow around cylinders with low aspect of ratio ($L/D < 6$) have been analyzed focusing on vortex shedding, as well as on the forces generated by the pressure field around the bodies. One of the pioneers in differentiating the fluid flow around the free end of cylinders with low aspect ratio was Kawamura *et al.* (1984) [13]. In that work, cylinders fixed at the

bottom were tested for the aspect ratio range of $1 \leq L/D \leq 8$; the authors observed an extensive effect on the vortex generated at the tip cylinder (called trailing vortex) and the usual von Kármán vortex street over the cylinder length. The influence noted for an aspect ratio was lower than $L/D_{crit} = 2.0$; this value was defined as the critical aspect ratio, in which the trailing vortex changed to the standard von Kármán street emission.

Before the work by Kawamura *et al.* (1984) [13], two major types of vortice structures formed behind bluff bodies had already been observed in Sakamoto & Arie (1983) [16] for cylinders with low aspect ratio. The first type was the well-known asymmetric and periodic vortex shedding von Kármán. The second shedding was specified with symmetric vortices, called arch-type vortices. The second wake behavior was predominant for values of aspect ratio lower than the critical aspect ratio as defined by $L/D_{crit} = 2.0$. The value of $L/D_{crit} = 2.5$ found by Sakamoto & Arie (1983) is similar to the value $L/D_{crit} = 2.0$ presented by Kawamura *et al.* (1984) [13].

The flow structure around the free end of a mounted finite circular cylinder with $L/D = 6$ was investigated experimentally by modifying the free-end corner shape in Park & Lee (2004) [14]. The authors concluded that the size of the recirculation bubble formed above the flat-tip finite cylinder tip is largely reduced by shaping the corner of the tip smoothly. The shear layer separating from the plain tip expands as the flow goes downstream, compared to the other tips tested. The turbulence intensity around the tip is also decreased as the tip is modified to a more streamlined shape.

The phenomenology around fixed cylinders can be used to better understand the behavior of 2 degrees of freedom (dof). For example, Gonçalves *et al.* (2015) [10] performed experiments on the flow around stationary circular cylinders with very low aspect ratio piercing the water free surface. Eight different aspect ratios were tested, $0.2 \leq L/D \leq 2.0$; no end-plates were employed. Forces were measured using a six-degree-of-freedom load cell, and the Strouhal number was inferred from the transverse force fluctuation frequency. The particle image velocimetry (PIV) measurements and the power spectrum density (PSD) of forces showed different behavior for cylinders with $L/D = 0.5$, in which cases the free-end effects were predominant. Even without von Kármán street main characteristics around the length of the cylinder, in the range of $0.2 < L/D \leq 0.5$, the vortex shedding around it was capable of producing alternating forces in the transverse direction. Therefore, alternating forces were not observed in the transverse direction for cylinders with $L/D \leq 0.2$.

Recently, Fukuoka *et al.* (2016) [5] performed similar experiments to evaluate the effects of the free surface and end cell on flow around a finite circular cylinder with low aspect ratio, and the results were similar as compared with the previous work cited for the aspect ratio tested $1 \leq L/D \leq 4$. Observations on flow around the fixed models produced important analyses for fluid dynamic field around cylinders with low aspect ratios. Using the PIV technology, both authors verified the occurrence of tip vortex, and its influence at the shedding formed at the cylinder walls.

The circular cylinder, or the bluff body, can experiment vortex-induced vibration (VIV) when free to oscillate and excited by a current flow. One demand of the offshore industry raised the interest in the VIV around cylinders with low aspect ratio ($0.30 < L/D < 6.00$) and small mass ratio ($m^* < 6.00$). This specific subject was called vortex-induced motion (VIM), and can be found in particular cases of spar ($1.50 < L/D < 6.00$) and monocolumn ($0.20 < L/D < 0.50$) platforms. Detailed VIM explanations can be found, for example, in Fujarra *et al.* (2012) [3].

Works about VIV of circular cylinders with low aspect ratio are few in the literature, among which Someya *et al.* (2010) [17], Gonçalves *et al.* (2012b [8], 2013 [9], 2018 [11]), Rahman & Thiagarajan (2013) [15], Fujiwara *et al.* (2013) [4], Zhao & Cheng (2014) [18] and Gambarine *et al.* (2016) [6] can be highlighted.

Gonçalves *et al.* (2018) [11] presented a series of fundamental results of VIV of floating circular cylinders with $0.2 \leq L/D \leq 2.0$. The amplitude results showed a decrease in amplitude with decreasing aspect ratio in the in-line and in the transverse directions. The frequency results confirm a different behavior for cylinders with $L/D \leq 0.5$; in these cases, the cylinder free-end effects were predominant. The resonant behavior was no longer observed for $L/D \leq 0.2$. The decrease in Strouhal number with decreasing aspect ratio is also verified, as well as for drag and lift forces. The amplitude results for the vertical direction, roll, pitch, and yaw did not affect the VIV behavior.

As a follow-up to the cited works, Gambarine *et al.* (2016) [6] carried out VIV experiments of cylinders with different free-end corner shapes in a towing tank for the same aspect ratio $L/D = 2.0$. The models were geometrically modified on edge immersed, implementing rounded chamfer at the cylinders tip, i.e. different values of r/R, where r is the radius of the corner edge and R is the half diameter of the cylinder. The aim was to observe the effect of the free-end corner shape $0.0 \leq r/R \leq 2.0$, on the VIV phenomenon considering the critical aspect ratio, $L/D_{crit} = 2.0$, as defined by Kawamura *et al.* (1984) [13]. The results showed similar amplitudes in the transverse direction for all the cases. These results concluded that the free-end effect for the aspect ratio tested, $L/D = 2.0$, did not affect the VIV behavior. Gonçalves *et al.* (2015 [10], 2018 [11]) showed that for a circular cylinder piercing the free surface, as discussed before, the free-end effects were predominant for $L/D = 0.5$; this statement is now the greatest motivation for the present study.

The present work focuses on the experimental study on the VIV of floating circular cylinders with aspect of ratio $L/D = 0.5$, value lower than the critical $L/D_{crit} = 2.0$, and four different free-end corner shape radius defined by the ratio $r/R = 0.0$, 0.25, 0.50 and 1.00. The goal is to understand the free-end effects for cylinders subjected to VIV when the structures generated around the free end are predominant and responsible for the forces that promote the motions.

Chapter 2 presents the experimental setup of the tests performed. Chapter 3 discusses the experimental results that comprise nondimensional amplitudes and frequencies in both

transverse and in-line direction as a function of the reduced velocity, $V_r = U/f_0 D$, as well as PSD for supporting the discussions and conclusions. Finally, chapter 4 draws the main conclusions and perspectives of the present work.

2. EXPERIMENTAL SETUP

All the experiments were carried out in a recirculating water channel at the Fluid & Dynamics Research Group Laboratory (NDF) facility of the University of São Paulo (USP), Brazil. The dimension of the test section is 7500x700x700mm, and the flow has low levels of turbulence (less than 2%). The pump system can operate with good quality with free-stream velocities up to 0.40m/s. Further details concerning the water channel can be found in Assi *et al*. (2006) [1].

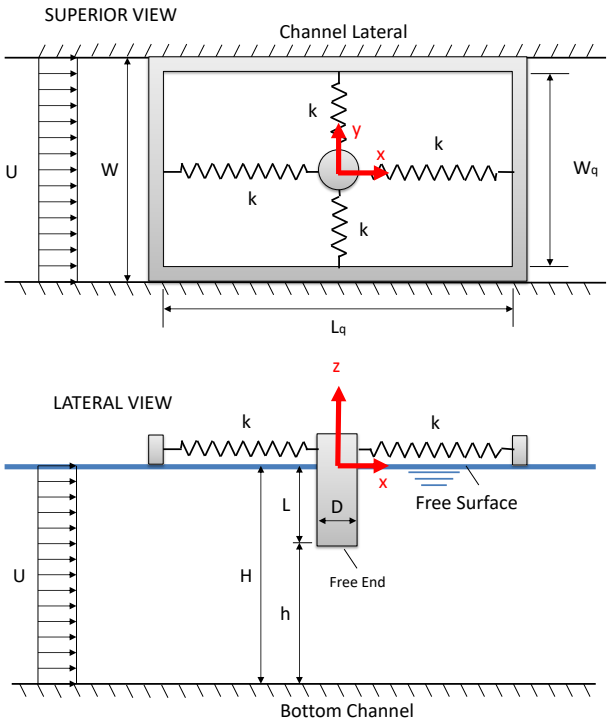

Figure 1 – Experimental setup and dimensional parameters.

The floating circular cylinder was elastically supported by a set of four springs with the same stiffness parameter, $k = 0.73$N/m, in rectangular support with dimensions $L_q = 1090$mm and $W_q = 610$mm, length and width respectively; as can be seen in Figure 1. The models were made of polyvinyl chloride (PVC) with external diameter D=125mm. The cylinder is free to move in the 6dof. The motions were measured using an optical motion capture system, Qualisys. Details can be seen in Figure 2.

Four different cylinders were built for each free-end corner shape configuration tested, namely: $r/R = 0.0$, 0.25, 0.50 and 1.00; see Figure 3 and Figure 4. The water height of the channel was kept constant during the tests, $H = 536$mm and the distance between the cylinder free-end and the bottom of the channel was $h = 474$mm.

The natural frequencies in still water in both directions were practically the same for each L/D condition, $f_{0x}/f_{0y} \sim 0.99$; due to this, it is possible to consider $f_{0x} = f_{0y} = f_0$. The damping coefficient in still water decreased by increasing the radius of the free-end corner shape, and were inferior to $\zeta_w \sim 4\%$ in all the cases. The structural damping was very low around $\zeta_s = 0.1\%$. The blockage effect coefficient was less than 2% for all the conditions performed.

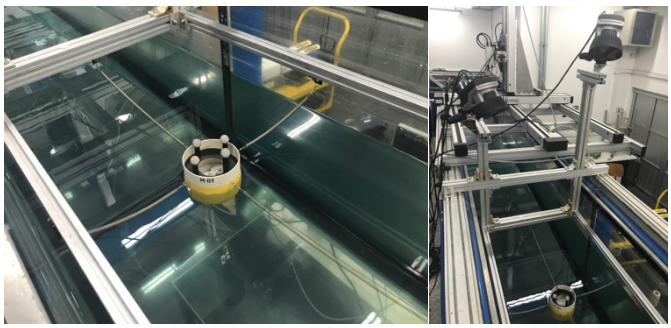

Figure 2 – Illustration of the floating cylinder elastically supported by a set of four springs and experimental arrangement of optical motion capture system.

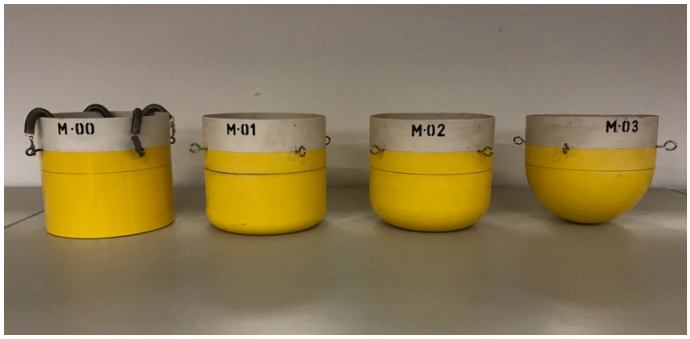

Figure 3 – Illustration of PVC models of the cylinders with low aspect ratio and different corner shapes.

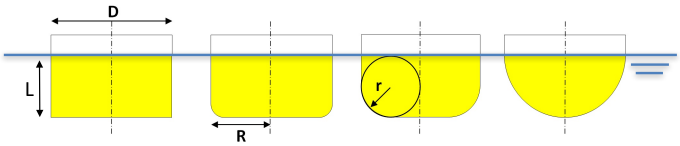

Figure 4 – Corner shape parameter details: (a) $r/R = 0.00$; (b) $r/R = 0.25$; (c) $r/R = 0.50$; (d) $r/R = 1.00$.

Forty velocity conditions were carried out for each free-end corner shape configuration. The reduced velocity range performed was $1 < V_r < 15$ and the Reynolds number range was $2 \times 10^3 < Re < 6 \times 10^4$, which corresponds to current incidences of $0.02 < U < 0.45$m/s.

Table 1 presents details about the conditions tested.

The 6dof were measured during the tests. The values of characteristic amplitudes in both directions, as well as the characteristic frequencies, were obtained employing the Hilbert-

Huang Transform Method (HHT) as proposed by Gonçalves *et al*. (2012a) [7].

Table 1 – Parameters of the tests for each corner shape condition.

r/R	$Re\ [\times 10^4]$	ζ_w [%]	$f_{0x} = f_{0y} = f_0$ $[Hz]$
0.00	0.29→5.10	3.19±0.13	0.22
0.25	0.30→5.06	2.52±0.10	0.23
0.50	0.50→5.28	2.31±0.05	0.24
1.00	0.67→5.45	1.94±0.05	0.28

3. EXPERIMENTAL RESULTS

Figure 5 and Figure 6, respectively, show the nondimensional amplitudes in the transverse and the in-line directions for the cases of $r/R = 0.0, 0.25, 0.50$ and 1.0.

The nondimensional amplitudes in the transverse direction, A_y/D, showed a distinct behavior for $r/R = 1.0$, see Figure 5. In this case, it was possible to observe the growth in amplitudes by increasing V_r, but it is not possible to observe the amplitude fall, which is one characteristic of the *lower branch*. On the other hand, the results showed a decrease of amplitudes for $V_r > 10$ for the cases of $0.0 \leq r/R \leq 0.5$. The values of nondimensional amplitudes in the transverse direction were always the highest for the semi-sphere case, $r/R = 1.0$, mainly in the region of $2 < V_r < 8$. All the cases presented the same transverse amplitude for $V_r \sim 8$. From $V_r > 8$, the increase in the radius of the free-end corner shape decreased the amplitudes. The transverse amplitude can confirm the effect of the free-end corner shape in the vortex-induced vibration of cylinders with very low aspect ratio. The structures around the cylinder free-end were responsible for generating the forces capable of moving the cylinder.

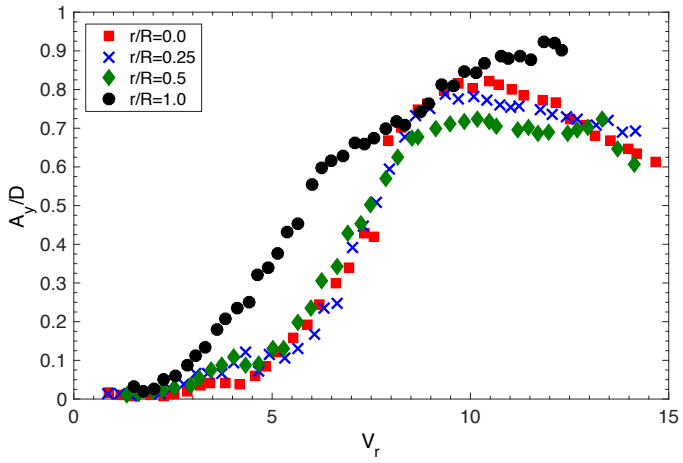

Figure 5 - Nondimensional motion amplitude in the transverse direction (A_y/D) as a function of reduced velocity (V_r) for cylinders with different free-end corner shapes.

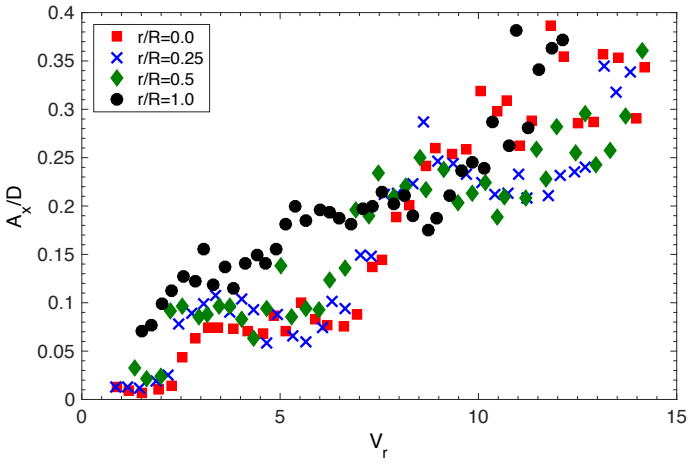

Figure 6 - Nondimensional motion amplitude in the in-line direction (A_x/D) as a function of reduced velocity (V_r) for cylinders with different free-end corner shapes.

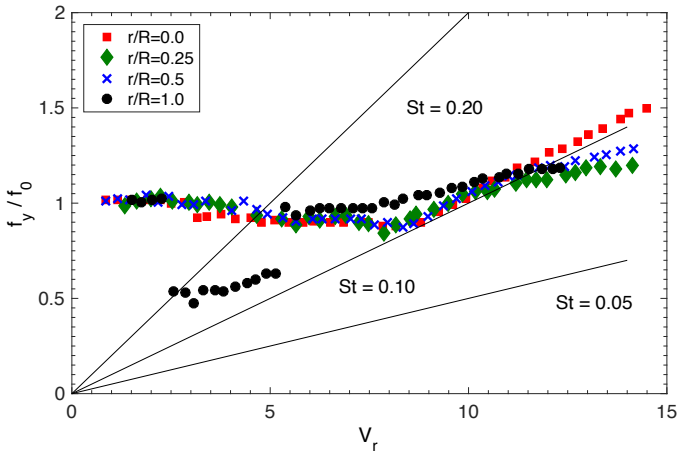

Figure 7 - Ratio between the transverse motion frequency and the natural transverse frequency in still water (f_y/f_0) as a function of reduced velocity (V_r) for cylinders with different free-end corner shapes.

Gambarine *et al.* (2016) [6] carried out similar previous experiments for $L/D = 2$. The results showed no difference between the cases tested with different free-end corner shapes, $r/R = 0.0, 0.25, 0.50$ and 1.0. The explanation was given by Gonçalves *et al.* (2015 [10], 2018 [11]), which discussed the structures around the free end of cylinders with $L/D \leq 0.5$, the main responsible for the transverse forces that promote the VIV. The present results, together the results by Gonçalves *et al.* (2015 [10], 2018 [11]) and Gambarine *et al.* (2016) [6] corroborate this affirmation and show the strong effect of the free-end corner shape on the VIV of circular cylinders with very low aspect ratio.

Govardhan & Williamson (2005) [12] performed tests on VIV of sphere. The motions in the transverse direction showed the same behavior as that presented here, an increase of the amplitudes by increasing the reduced velocity and an absence of decrease in amplitudes even for high values of reduced velocity for small mass ratio cases $m^* \leq 1$. This comparison can help to explain the structures around the free-end for $r/R = 1.0$.

The nondimensional amplitudes in the in-line direction, A_x/D, also showed a distinct behavior for $r/R = 1.0$, see Figure 6. In this case, the in-line amplitudes were the highest for most of the reduced velocity range. For the other cases, $0.0 \leq r/R \leq 0.5$, one first local maximum was found around $V_r \sim 3$ and a linear increase of amplitudes for $V_r > 6$ and similar maximum values for this range of radius. The amplitude results had a large dispersion after $V_r > 10$ due to the high value of the cylinder drift for these conditions.

The results of ratio between the transverse motion frequency and the natural transverse frequency in still water, f_y/f_0, presented in Figure 7 also showed a different behavior for the case $r/R = 1.0$. A linear increase of f_y/f_0 as a function of V_r occurred for $V_r > 7$ and $0.0 \leq r/R \leq 0.5$. In this region, it is possible to assume that the vortex shedding frequency is similar to the motion frequency in the transverse direction, $f_s \cong f_y$, making it possible to infer the Strouhal number as the curve inclination. Additionally, a constant value of $f_y/f_0 \sim 0.9$ to $V_r \sim 7$ for $0.0 \leq r/R \leq 0.5$ was observed. The Strouhal number was around $St \sim 0.10$ for $r/R = 0.0$, the same presented in Gonçalves *et al.* (2018) [11]. For $r/R = 0.25$ and $r/R = 0.50$, the curve inclination was lower than $r/R = 0.00$, which showed the different frequency shedding of the structures around the rounded edge in these cases.

It is hard to understand the ratio of frequencies when the motion is not harmonic, i.e. there is more than one characteristic frequency. This behavior was observed for the in-line motions. PSD results were evaluated to try to better visualize the frequency components presented in each reduced velocity for the motions in the in-line and transverse directions, as presented in Figure 8 and Figure 9.

The PSD results of the motions in the in-line direction see Figure 8, showed two regions where the dominant in-line frequency is defined. The first region, $V_r < 7$, is characterized by a constant value $f_x/f_0 \sim 1$; and the second region, $V_r > 7$, is characterized by an inclined line when looking at the graph of f_x/f_0 as a function of V_r, and also by a line with constant value when looking at the graph of $f_x D/U$ as a function of V_r. It was possible to observe that the range of the first region decreased by decreasing the free-end corner shape radius. Moreover, the highest energy level for the motions in the in-line direction in the first region is observed for the semi-sphere case. On the other hand, the energy in the second region increased by decreasing the free-end corner shape radius.

The PSD results of the motions in the transverse direction, see Figure 9, showed the region where the dominant transverse frequency is defined. This region, $V_r > 7$, is also characterized by an inclined line, practically with half the inclination verified in the in-line direction, when looking at the graph of f_x/f_0 as a function of V_r, and also by a line with constant value, practically half as that verified in the in-line direction, when looking at the graph of $f_x D/U$ as a function of V_r. These values characterize

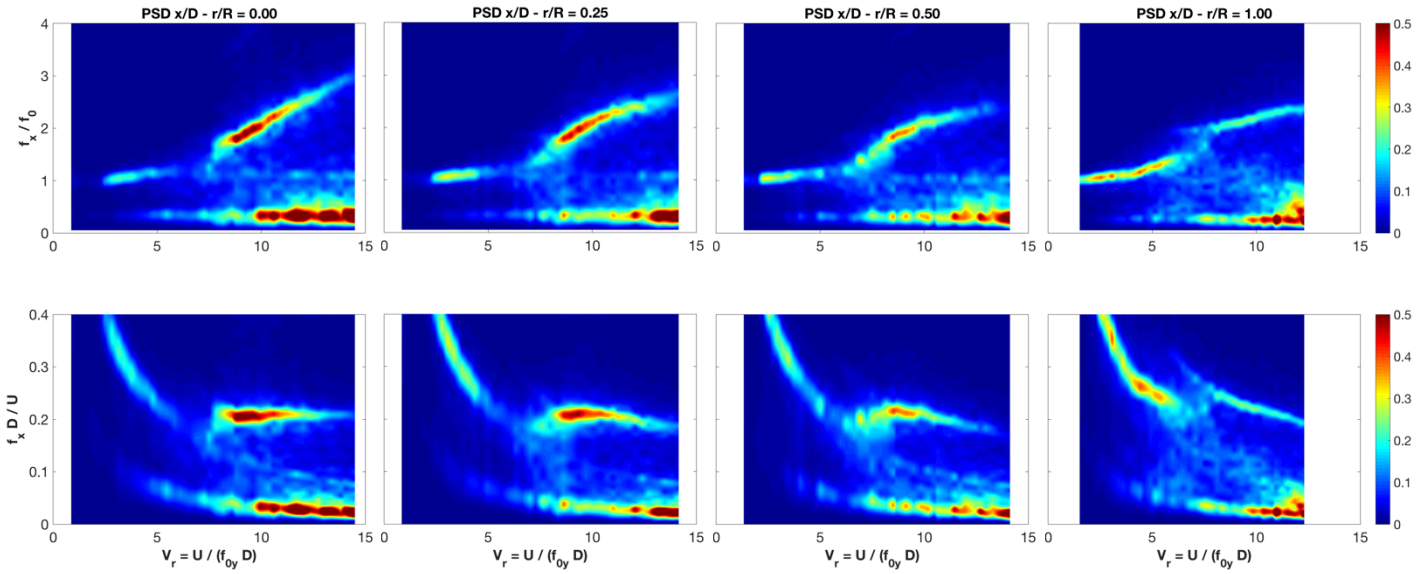

Figure 8 – PSD of the motion in the in-line direction as a function of V_r for cylinders with mass ratio of $m^* = 1.00$ and different aspect ratios ($1.00 \leq L/D \leq 2.00$). The dimension of the color scale is 1.s.

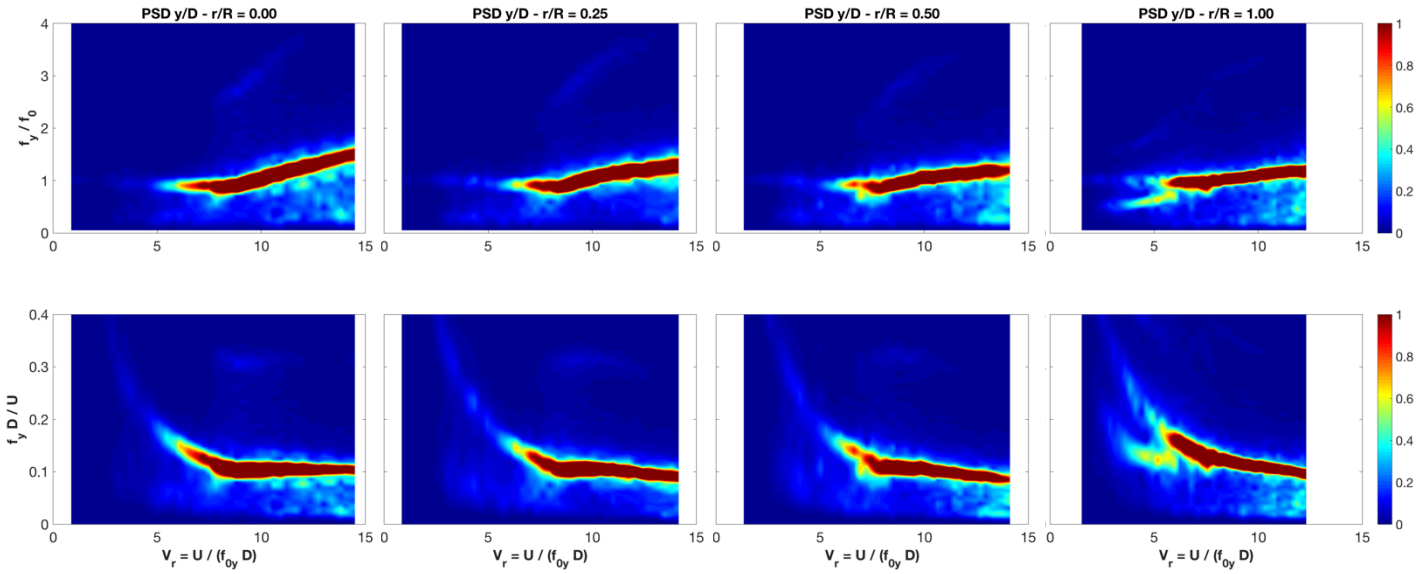

Figure 9 – PSD of the motion in the transverse direction as a function of V_r for cylinders with mass ratio of $m^* = 1.00$ and different aspect ratios ($0.20 \leq L/D \leq 0.30$). The dimension of the color scale is 1.s.

the Strouhal number for each free-end corner shape radius condition assuming that the vortex shedding frequency is similar to the motion frequency in the transverse direction, $f_s \cong f_y$.

In the same way as in the in-line direction, it was possible to observe that in this range, the line inclination, or Strouhal number, decreased by increasing the free-end corner shape radius. Moreover, for $r/R = 1.0$, it was possible to observe energy with low frequency for $V_r < 7$, behavior not presented when compared with the lower radius values. These results contributed to showing that the structures around the cylinder free end were different for the semi-sphere case. Govardhan & Williamson (2005) [12] showed that the Strouhal number for the sphere case is around 0.05, which is similar to the value observed herein.

Figure 10 presents the mean pitch angle results in function of the reduced velocity. Due to the largest area exposed to the flow, the case of $r/R = 0.00$ presented the largest mean pitch value when compared with the other cases; and the semi-sphere

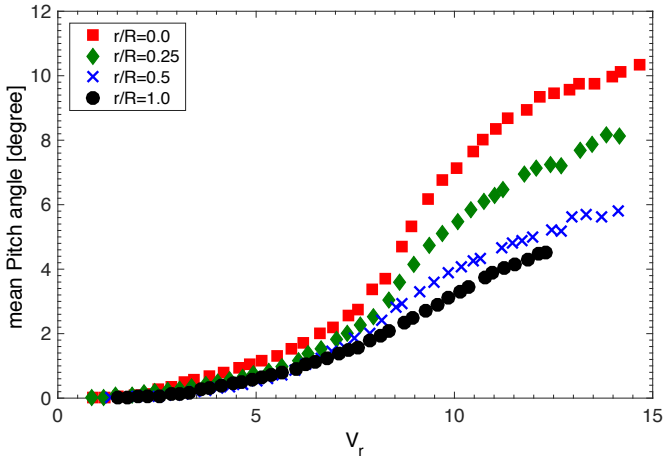

Figure 10 – Mean pitch angle as a function of reduced velocity (V_r) for cylinders with different free-end corner shapes.

case, $r/R = 1.00$, presented the lowest one. These results showed that the mean pitch angle is not large enough to affect the structures around the free-end and be responsible for the different behavior of the different corner shape radius. The results of the mean pitch angle for $r/R = 0.50$ and $r/R = 1.00$ were quite similar, lower than 6 degrees for all the reduced velocities tested; conversely, the nondimensional amplitudes in the transverse direction in Figure 5 were completely different. This comparison helps to demonstrate that the pitch angle and the transverse motions amplitudes were not correlated. Franzini *et al.* (2013) [2] discussed the yaw angle effects on the VIV of circular cylinders; the results showed that the effect could be neglected for angles lower than 10 degrees.

4. GENERAL CONCLUSIONS

The present work was motivated by the previous VIV studies carried out by Gambarine *et al.* (2016) [6] and Gonçalves *et al.* (2018) [11]. VIV experiments were thus carried out in a circulating water channel at NDF to verify the effects of the free end on the VIV of floating circular cylinders with very low aspect ratio. Four different conditions of free-end corner shape radius were tested, namely $r/R = 0.0$, 0.25, 0.50 and 1.00. In all the conditions, the cylinder was free to oscillate with 6dof, $m^* = 1$ and $L/D = 0.5$. Motions were acquired utilizing an optical motion capture system. Results regarding motion amplitudes and motion characteristic frequencies were presented and discussed for each corner radius value.

Regarding the motion amplitudes, the nondimensional amplitudes in both directions were the highest for the semi-sphere case, $r/R = 1.00$. The nondimensional amplitude behaviors were practically the same for the other radius values, $0.0 \leq r/R \leq 0.5$; the difference was observed in the high reduced velocity range $V_r > 7$, in which the maximum amplitudes decreased by increasing the corner radius.

The frequency results showed a decrease in the Strouhal number by increasing the corner radius. Moreover, energy in lower frequencies was observed for the semi-sphere case when compared with other cases. Thus, it is possible to argue that low-frequency structures become important when increasing the corner radius.

The present work, together with the results by Gambarine *et al.* (2016) [6] helped to confirm the statement by Gonçalves *et al.* (2015 [10], 2018 [11]) in which the structures around the cylinder free end are predominant for aspect ratio lower than $L/D = 0.5$; therefore, this value can be considered the critical value, $L/D_{crit} = 0.5$, in which only the free-end structures affect the VIV behavior of the cylinder piercing the free-surface.

Future works are being conducted to visualize the structures around the free-end. PIV measurements can help to better understand the behavior, besides providing new conclusions. Different free-end geometries, such as the inclusion of different diameter end plates, can be considered.

NOMENCLATURE

ζ_s	structural damping
ζ_w	damping coefficient in still water
A_x/D	characteristic nondimensional motion amplitude in the in-line direction
A_y/D	characteristic nondimensional motion amplitude in the transverse direction
D	characteristic diameter
f_0	natural frequency in still water, both in in-line and transverse directions
f_{0x}	natural frequency of the system in still water in the in-line direction
f_{0y}	natural frequency of the system in still water in the transverse direction
f_s	vortex-shedding frequency
f_x	oscillation frequency in the in-line direction
f_y	oscillation frequency in the transverse direction
h	distance between the cylinder free-end and the bottom of the channel

H	water height of the channel
k	spring stiffness parameter
L	immersed length
L_q	length of the model support
m^*	mass ratio
m_d	displaced mass
m_s	structural mass
$L\ /\ D$	aspect ratio
r	chamfer rounding radius
R	radius of the cylinder
r/R	corner shape radius ratio
Re	Reynolds number
U	flow velocity
V_r	reduced velocity
W	width of the water channel
W_q	width of the model support

ACKNOWLEDGMENTS

The authors would like to acknowledge The Japan Society of Naval Architects and Ocean Engineers (JASNAOE) for the financial support of the internship period of the Japanese students in Brazil when the model was tested, and the Numerical Offshore Tank Laboratory (TPN) at the University of São Paulo (USP) for hosting the students.

REFERENCES

1. ASSI, G. R. S., MENEGHINI, J. P., ARANHA, J. A. P., BEARMAN, P. W. & CASAPRIMA, E. Experimental investigation of flow-induced vibration interference between two circular cylinders. *Journal of Fluids and Structures*, Vol. 22, pp. 819-827, 2006.

2. FRANZINI, G. R., GONÇALVES, R. T., MENEGHINI, J. R. & FUJARRA, A. L. C. One and two degrees-of-freedom vortex-induced vibration experiments with yawed cylinders. *Journal of Fluids and Structures,* Vol. 42, pp. 401-420, 2013.

3. FUJARRA, A. L. C., ROSETTI, G. F., WILDE, J. & GONÇALVES, R. T. State-of-art on vortex-induced motion: A comprehensive survey after more than one decade of experimental investigation. In: *Proceedings of the 31st International Conference on Ocean, Offshore and Arctic engineering*, OMAE2012-83561. Rio de Janeiro, Brazil, 2012.

4. FUJIWARA, T., SAITO, M., MAEDA, K., SATO, H. & ISHIDA, K. Experimental investigation of VIM characteristics on column type floater in super critical Reynolds number. In: *Proceedings of the 32nd International Conference on Ocean, Offshore and Arctic Engineering*, OMAE2013-10473. Nantes, France, 2013.

5. FUKUOKA, H., HIRABAYASHI, S. & SUZUKI, H. The effects of free surface and end cell on flow around a finite circular cylinder with low aspect ratio. *Journal of Marine Science and Technology*, Vol. 21(1), pp. 145-153, 2016.

6. GAMBARINE, D. M., FIGUEIREDO, F. P., FUJARRA, A. L .C. & GONÇALVES, R. T. Experimental study about the influence of the free end effects on vortex-induced vibration of floating cylinder with low aspect of ratio. In: *Proceedings of the 35th International Conference on Ocean, Offshore and Arctic engineering*, OMAE2016-54632. Busan, South Korea, 2016.

7. GONÇALVES, R. T., FRANZINI, G. R., ROSETTI, G. F., FUJARRA, A. L. C. & NISHIMOTO, K. Analysis methodology for vortex-induced motion (VIM) on a monocolumn platform applying the Hilbert-Huang transform method. *Journal of Offshore Mechanics and Arctic Engineering*, Vol. 134, pp. 011103-1-7, 2012a.

8. GONÇALVES, R. T., ROSETTI, G. F., FUJARRA, A. L. C., FRANZINI, G. R., FREIRE, C. M. & MENEGHINI, J. R. Experimental comparison of two degrees-of-freedom vortex-induced vibration on high and low aspect ratio cylinders with small mass ratio. *Journal of Vibration and Acoustics*, Vol. 134, pp. 061009-1-7, 2012b.

9. GONÇALVES, R. T., ROSETTI, G. F., FRANZINI, G. R., MENEGHINI, J. R. & FUJARRA, A. L. C. Two degrees-of-freedom vortex-induced vibration of circular cylinders with very low aspect ratio and small mass ratio. *Journal of Fluids and Structures*, Vol. 39, pp. 237-257, 2013.

10. GONÇALVES, R. T., FRANZINI, G. F., ROSETTI, G. F., MENEGHINI, J. R. & FUJARRA, A. L. C. Flow around circular cylinders with very low aspect ratio. *Journal of Fluids and Structures*, Vol. 54, pp. 122-141, 2015.

11. GONÇALVES, R. T., MENEGHINI, J. R. & FUJARRA, A. L. C. Vortex-induced vibration of floating circular cylinders with very low aspect ratio. *Ocean Engineering,* Vol. 154C, pp. 234-251, 2018.

12. GOVARDHAN, R. N. & WILLIAMSON, C. H. K. Vortex-induced vibrations of a sphere. *Journal of Fluid Mechanics*, Vol. 531, pp. 11-47, 2005.

13. KAWAMURA, T., HIWADA, M., HIBINO, T., MABUCHI, I. & KUMADA, M. Flow around a finite circular cylinder on a flat plate. *Bulletin of the Japan Society of Mechanical Engineers*, Vol.27, pp. 2142-2151, 1984.

14. PARK, C. W. & LEE, S. J. Effects of free-end corner shape on flow structure around a finite cylinder. *Journal of Fluids and Structures*, Vol. 19, pp. 141-158, 2004.

15. RAHMAN, M. A. A. & THIAGARAJAN, K. Vortex-induced vibration of cylindrical structure with different aspect ratio. In: *Proceedings of the 17th International*

Offshore and Polar Engineering Conference. Alaska, USA, 2013.

16. SAKAMOTO, H. & ARIE, M. Vortex shedding from a rectangular prism and a circular cylinder placed vertically in a turbulent boundary layer. *Journal of Fluid Mechanics*, Vol. 126, pp. 147-165, 1983.

17. SOMEYA, S., KUWABARA, J., LI, Y. & OKAMOTO, K. Experimental investigation of a flow-induced oscillating cylinder with two degrees-of-freedom. *Nuclear Engineering and Design*, Vol. 240, pp. 4001-4007, 2010.

18. ZHAO, M. & CHENG, L. Vortex-induced vibration of a circular cylinder of finite length. *Physics of Fluid,* Vol. 26, pp. 015111, 2014